# Gravitational Wave Detection: Principles and Practice

Peter R. Saulson

Department of Physics, Syracuse University, Syracuse, NY 13244, USA

October 2, 2011

## ABSTRACT

The technology of gravitational wave detection has been developed to a high degree. I review the basic principles of interferometric detectors, and give an account of the current state of the art, and plans for the near term future.

# 1 What are gravitational waves, and how can they be detected?

Einstein predicted the existence of gravitational waves as part of his development of the general theory of relativity.[1] It made deep physical sense for a relativistic theory of gravity to include waves in the gravitational field (or, in relativistic language, in the curvature of space-time); after all, the deepest idea of relativity is that no information may be transmitted (by any means) any faster than the speed of light. Without gravitational waves, general relativity would have reproduced the instantaneous action-at-a-distance of Newton's theory of gravity. This would allow (in principle at least) the construction of a gravitational signaling system that violated relativistic causality. General relativity leads to a wave equation in which re-arrangements of mass cause weak perturbations in empty space that travel as waves at the speed of light.

Given the importance of gravitational waves for the intellectual coherence of general relativity, it is somewhat surprising that Einstein himself was among those who doubted the physical reality of gravitational waves.[2] One of the subtleties of general relativity is the difficulty of distinguishing between genuine physical phenomena and those that only appear because of the particular choice of coordinates used to describe the system. In an article of 1922,[3] Eddington coyly reports that there are those who think that gravitational waves travel, not at the speed of light, but at the "speed of thought." Kennefick recounts the story of Einstein and Rosen having written a paper in 1936 claiming to prove that gravitational waves were "pure gauge", and having submitted it to Physical Review. The referee strongly critiqued the article, and the authors were asked to respond to his criticisms. Einstein, not used to how refereed journals worked, haughtily withdrew the paper rather than replying to the referee. In the process of revising the paper for submission to the non-refereed *Journal of the Franklin Institute*, Einstein was persuaded by H.P. Robertson that the original argument was flawed, and the published version of the paper[4] makes no claim about the non-existence of gravitational waves.

The episode indicates that relativity is subtle, even for its founder.

The confusion about the physical reality of gravitational waves was only resolved in 1957. The credit is usually given to Hermann Bondi and his "sticky bead" argument.[5] Others give credit to Richard Feynman, who at the Chapel Hill Conference[6] in 1957 was in fact the first to describe how a gravitational wave could cause motion of beads along a sticky rod, and thus deposit heat in the apparatus. But credit should actually be given to Bondi's former student and by-then colleague Felix Pirani, who gave a much clearer and more complete explanation of the physics earlier in the Conference, based on papers that he had submitted to journals months before.[7] This specific result was a product of a program that Pirani carried out to show that the physically meaningful effects of gravitation in general relativity could be observed as relative accelerations between neighboring free masses. One particularly interesting special case was the application to the question of the detectability (and thus the physical reality) of gravitational waves. Pirani's paper at the Chapel Hill Conference, and the exchange between Pirani and Bondi that immediately follows it in the Proceedings, show the issue being worked out completely.

One might even suspect that Pirani's paper was the direct inspiration for the entire program to detect gravitational waves.[8] Joseph Weber was present at Chapel Hill, and was interested in precisely these questions. Rainer Weiss, the inventor of what became LIGO, was not at the Chapel Hill Conference, but he did carefully study the published
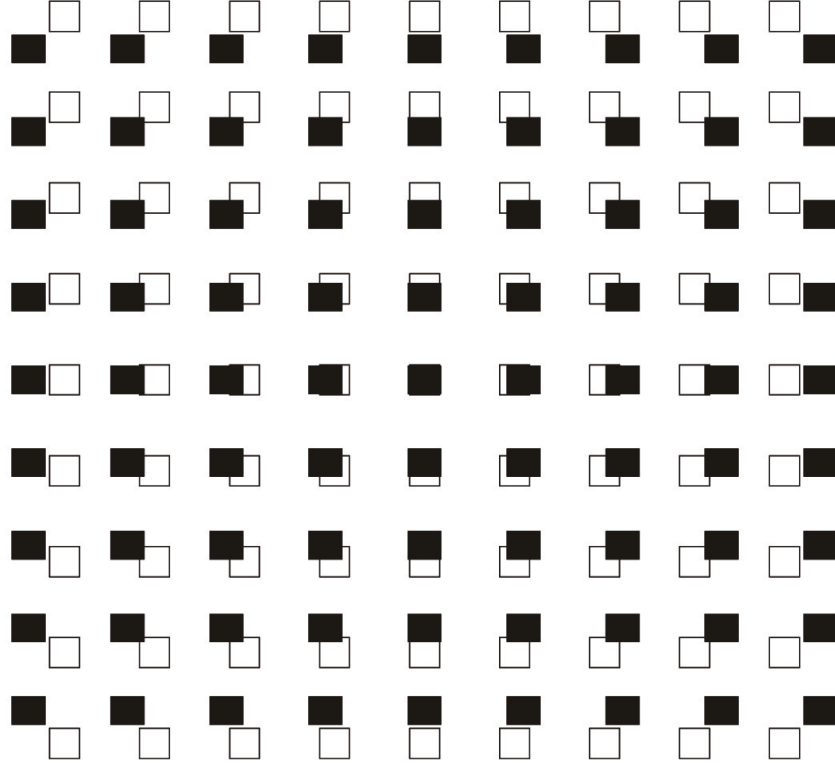
Figure 1: A gravitational wave causes a set of free masses to change their separations from one another in a pattern like the one shown here. Open squares represent the original positions of the masses, while the filled squares represent their instantaneous relative positions while a gravitational wave of polarization $h_+$ is present.

versions of Pirani's paper in the process of proposing the construction of interferometric gravitational wave detectors.[9]

What was it that Pirani taught to Bondi, Feynman, Weber, and Weiss?

A gravitational wave is a solution of the Einstein equations in the weak field limit. The physically meaningful effect (in Pirani's sense) is a transverse traceless wave that travels at the speed of light. Transverse waves are, of course, familiar from our study of electromagnetic waves. "Traceless" means that the waves have equal and opposite effects in two perpendicular directions. Thus, a wave traveling in the $\hat{z}$ direction causes measurable relative motion in the $\hat{x}$ and $\hat{y}$ directions between sets of neighboring free masses, with motions in the $\hat{y}$ direction equal and opposite to those in the $\hat{x}$ direction. This pattern is shown in Figure 1. These are real physical motions that can stretch a spring or cause friction in a dashpot.

More formally, we can describe a gravitational wave traveling through otherwise flat space by the metric

$$g_{\mu\nu} = \eta_{\mu\nu} + h_{\mu\nu} \tag{1}$$

where, for the special case of a wave traveling along the $\hat{z}$ axis, the metric perturbation can

be written as

$$h_{\mu\nu} = \begin{pmatrix} 0 & 0 & 0 & 0 \\ 0 & a & b & 0 \\ 0 & b & -a & 0 \\ 0 & 0 & 0 & 0 \end{pmatrix}. \tag{2}$$

In other words, we can write this wave as a sum of two components, $h = a\hat{h}_+ + b\hat{h}_\times$, with

$$\hat{h}_+ = \begin{pmatrix} 0 & 0 & 0 & 0 \\ 0 & 1 & 0 & 0 \\ 0 & 0 & -1 & 0 \\ 0 & 0 & 0 & 0 \end{pmatrix}, \tag{3}$$

and

$$\hat{h}_\times = \begin{pmatrix} 0 & 0 & 0 & 0 \\ 0 & 0 & 1 & 0 \\ 0 & 1 & 0 & 0 \\ 0 & 0 & 0 & 0 \end{pmatrix}. \tag{4}$$

The "basis tensors" $\hat{h}_+$ and $\hat{h}_\times$ (pronounced "h plus" and "h cross") represent the two orthogonal polarizations for waves propagating along the $\hat{z}$ axis.

As Pirani emphasized in the *Acta Physica Polonica* paper that influenced Weiss, those physical motions can be sensed as changes in the (round trip) light travel time between the masses. Weiss saw how a Michelson interferometer was perfectly suited for sensing a transverse traceless wave; a Michelson interferometer compares the light travel time in the two arms, so the opposite effects in $\hat{x}$ and $\hat{y}$ directions combine to increase the signal at the output.

We can carry out Pirani's program explicitly, as Weiss did, by starting with the basic fact from relativity that the interval between any two events on the path of a beam of light is described simply by $ds^2 = 0$

Let the arms of a Michelson interferometer be laid out along the $\hat{x}$ and $\hat{y}$ axes, with the beam-splitter at the origin. It is handy to first consider the light that travels in the $\hat{x}$ arm. It is governed by

$$\begin{aligned} ds^2 = 0 &= g_{\mu\nu}dx^\mu dx^\nu \\ &= (\eta_{\mu\nu} + h_{\mu\nu})dx^\mu dx^\nu \\ &= -c^2 dt^2 + (1 + h_{11}(2\pi ft - \vec{k}\cdot\vec{x}))dx^2. \end{aligned} \tag{5}$$

Pirani taught us that this can be interpreted as a modulation of the distance between neighboring points of fixed coordinate separation $dx$ (as marked by freely falling masses) by an amount $h_{11}$. To see how this is observable as an effect on light travel time, we rearrange the equation to find

$$\int_0^{\tau_{out}} dt = \frac{1}{c}\int_0^L \sqrt{1 + h_{11}}\, dx \approx \frac{1}{c}\int_0^L (1 + \frac{1}{2}h_{11}(2\pi ft - \vec{k}\cdot\vec{x}))dx, \tag{6}$$

where we've used the binomial expansion to simplify the square root. A similar expression can be written for the return trip from the x-end mirror back to the beam splitter, and we can add the two expressions to find

$$\tau_{rt} = \frac{2L}{c} + \frac{1}{2c}\int_0^L h_{11}(2\pi ft - \vec{k}\cdot\vec{x})dx - \frac{1}{2c}\int_L^0 h_{11}(2\pi ft - \vec{k}\cdot\vec{x})dx. \tag{7}$$

3

We can write a similar expression for the light that travels through the $\hat{y}$ arm. The only difference is that it involves $h_{22}$ instead of $h_{11}$. An interferometer's output depends on the difference in light travel time between the two arms. The method sketched here lets us calculate the travel time difference for arbitrary signal frequencies and sky positions. But for purposes of building intuition, consider the special case of a wave arriving from the $\hat{z}$ direction, and with $2\pi f \tau_{rt} \ll 1$. This special direction of arrival makes $h_{11} = -h_{22} = h$, while the low frequency means that the gravitational wave $h(t)$ is constant throughout the propagation of light through the interferometer arms. In this important special case, we can see that the travel time difference between the two interferometer arms is

$$\Delta\tau(t) = h(t)\frac{2L}{c} = h(t)\tau_{rt0}, \tag{8}$$

or that the optical phase difference between the two arms is

$$\Delta\phi(t) = h(t)\tau_{rt0}\frac{2\pi c}{\lambda}, \tag{9}$$

where $\lambda$ is the wavelength of the laser light. This says that the phase shift between the light that traveled in the two arms is equal to a fraction $h$ of the total phase that a light beam accumulates as it traverses the apparatus.

The low frequency response as a function of arbitrary angle, or beam pattern, is[10]

$$\Delta\phi(t) = h(t)\tau_{rt0}\frac{2\pi c}{\lambda}(\frac{1}{2}(1+\cos^2\Theta)\cos 2\Phi \cos 2\Psi - \cos\Theta\sin 2\Phi\sin 2\Psi), \tag{10}$$

where $\Theta$ and $\Phi$ are the polar and azimuthal angles, and $\Psi$ is the polarization angle of the wave. This pattern (averaged over polarization) is illustrated in Figure 2.

This pattern is remarkably isotropic, with a very large range of angles within a factor of two of the maximum sensitivity. This is of crucial importance for gravitational wave searches with a worldwide network. Our large interferometers cannot be pointed, but instead must be installed in a close approximation to level at each site around the world. Thus each "points" in a different direction. Nevertheless, because the beam pattern is so close to uniform, we can consider each interferometer to be scanning a very large portion of the entire sky. (The deviations from perfect isotropy are important complications in gravitational wave searches, but the basic point still holds.)

But if interferometers don't "point", how can we tell from where in the sky a signal has arrived? Simultaneous observations at multiple interferometers around the globe holds the key. One straightforward way to determine sky position is to record the time of arrival of a signal at each interferometer in the network. Detection at two sites with separation $D$ allows one to determine one time difference, defining a circle on the sky at an angle

$$\Theta = \arcsin\frac{c\Delta t}{D}, \tag{11}$$

as measured from one end of the line connecting the two sites. Detection at three sites determines two intersecting circles on the sky, yielding two (separate) error boxes. Detection at a fourth site would give the position unambiguously.

There is more information that can be extracted than simply time of arrival, giving other possible ways to learn more. So-called "coherent" methods aim to do this. They search a complete grid of sky positions, seeking to determine a combination of two waveforms $h_+(t)$ and $h_\times(t)$ and sky position that best explains the set of observations.[11],[12]
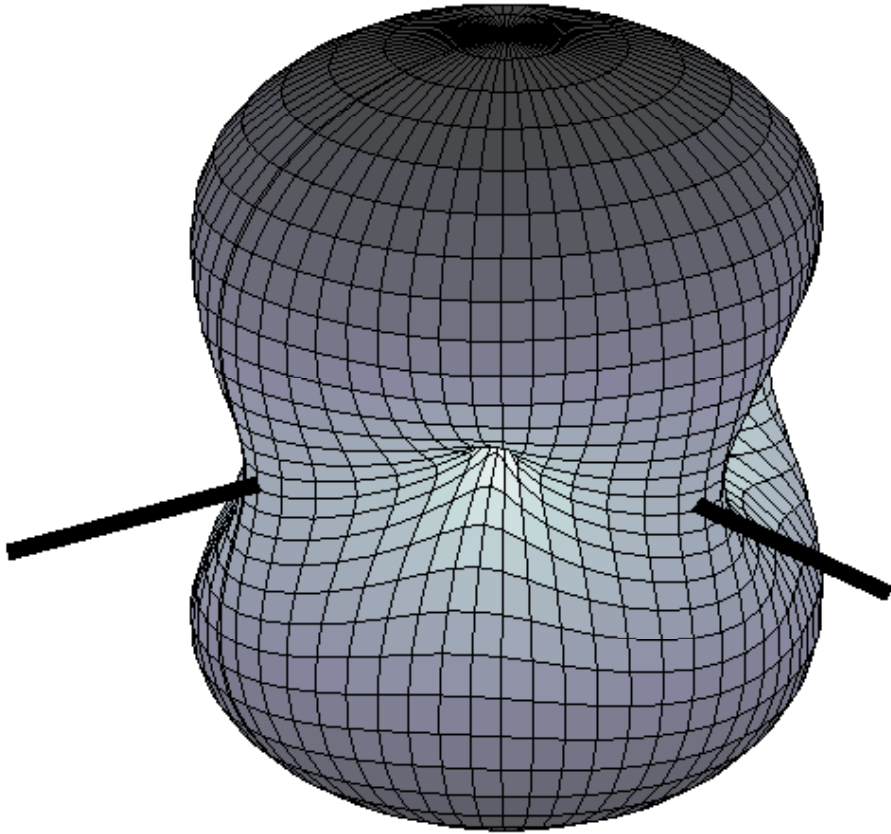
4

Figure 2: Response of a gravitational wave interferometer as a function of direction, averaged over polarizations.

# 2   Noise Sources

The previous section dealt with the intellectual difficulty of gravitational wave detection. There is also a tremendous practical difficulty – the signals that will be presented to a gravitational wave detector are extremely small, strain amplitudes of the order of $10^{-22}$.[13] Even with test mass separations of several km, this small strain translates into relative motions that are minuscule, a few times $10^{-19}$ meters.

The consequence of such a small signal is that the practice of gravitational wave detection calls for experimental strategies that are in many ways unprecedented in the history of physical measurement. In this section, we will look at that fundamental limits to the precision of measurements of mechanical strains. Important considerations include the size and optical configuration of an interferometer, the limit to precision of the readout of an interferometer, mechanical noise sources of various kinds, and a host of "technical" noise sources that come from the way in which the state of the interferometer is sensed and controlled.

For a more detailed discussion than can be given in this review, readers are referred to the author's *Fundamentals of Interferometric Gravitational Wave Detectors*[14] (now rather dated), and to the brand-new and very complete *Gravitational-Wave Physics and Astronomy* by Creighton and Anderson.[15]

## 2.1   The question of "free masses"

So far, we've blithely referred to the use of "free masses", as if that were something easy to include in a gravitational wave detector. It isn't; but it is possible to design a sufficiently good imitation for most purposes.

The mirrors obviously cannot be truly free, since a freely-falling mirror soon hits the floor of the laboratory and breaks. The mirrors must be held in place (for this and many other reasons!), but nevertheless behave as if free in some meaningful sense. This is accomplished, first and foremost, by suspending them from fine wires as pendulums. This gives most of what one might want. Most obviously, the masses are held at a fixed mean position within the apparatus. Nevertheless, the soft suspension allows motion in response to gravitational effects. Here's a way to see how it works: The equation of motion of a suspended mass is

$$m\ddot{x} + kx = F_{ext}. \tag{12}$$

In the frequency domain, this is equivalent to

$$-m(2\pi f)^2 x + kx = F_{ext}. \tag{13}$$

If a signal has its frequency high compared to the resonant frequency $f_0 = \sqrt{k/m}/(2\pi)$, then the term that comes from the inertia of the mass dominates, and it is as if the spring wasn't there at all. In other words, the mass behaves as a free mass at high frequencies, even though it is held in place. Nice trick!

Below, we'll see why a pendulum is the universal choice for test mass suspension, instead of some other form of mechanical suspension. Here, though, it is important to underline a major price that is paid for using this (or any other) form of suspension. Interferometers only work when:

- the light beams are well aligned with each other, so that they overlap (and do so in a very steady way), and

- the arm lengths are (and remain) very closely matched, with a steady average phase relationship. Obviously, we need to allow that phase relationship to vary above some frequency in order to be sensitive to gravitational waves, but it needs to do so by small amounts, about a steady average value.

In order to achieve these requirements, the inventor of the Michelson interferometer lavished great care on rigid mounts for all of the mirrors, as can be seen by studying the illustrations in the 1887 paper.[16]

We need to reproduce the key features of rigid mounting of mirrors, without the rigidity. In gravitational wave interferometers, this is accomplished by the use of feedback control systems to hold all crucial degrees of freedom (both in position and in angle) at the required operating points. This is beautiful (and challenging) technology. The most beautiful feature (for our purpose) is that it is quite natural to implement a control system that simulates rigidity at the low frequencies where rigidity is required, while allowing for freedom at the higher frequencies (above, say, a few tens of hertz) where freedom is required. The challenges are several, as will be described below: generation of the proper "error signal" as a measure of distance from the chosen operating point; low enough noise to not swamp the weak signals that we are seeking; and avoidance of instability. Interested readers are referred to the specialized literature for a more in-depth treatment of these issues than can be provided in this review.

## 2.2 Scale of detectors

As mentioned above, interferometers have been built on kilometer length scales, in order to make the signal as large as possible. (See below for details of the various large interferometer projects.) Long arms are expensive, and those that were built were the most expensive that the sponsors could afford. But none of them are the optimal length. A lesson from Eq. 9 above is that signal continues to grow with the length of the arm, up until the point that light spends time in the arm comparable to (one half of) the period of the gravitational wave. (After such a time, a sign reversal in the wave means that the signal will no longer accumulate from additional time in the arm.)

It is, in fact, possible to create an optical path of the required length within an arm whose physical length is too short. Michelson and Morley first did this in their famous 1887 paper; adding mirrors to fold a much longer path onto a table of fixed size, they were able to increase their sensitivity to a putative "ether drift" signal to the point that they were able to make a clear non-detection statement, while Michelson's first attempt in 1881, with only a simple Michelson interferometer, had failed.[17]

GEO 600 uses a simple version of the Michelson-Morley folding scheme to lengthen its arms by a factor of two, to a round-trip length of 2.4 km. The other large projects use a sophisticated form of Fabry-Perot resonant optical cavity. (This is one of the several key design features introduced by Ron Drever.[18]) Instead of requiring separate mirrors for each "bounce" (or single large mirrors as in a Herriott delay line,[19]) single (relatively small) mirrors at each end are arranged so that their separation is very close to an integer number of half-wavelengths of the light in the arm. Then, an optical resonance occurs, in effect trapping the light for many round trips. The effective number of round trips is of order the finesse of the cavity resonance. The finesse is determined by the finite transmission of the input mirror (necessary to allow light to move into and out of the cavity) as well as by any losses in the mirrors. Finesse of order 100 allows optimization of optical path length down to about 100 Hz in 3-4 km arms.

The Fabry-Perot solution has one key advantage: the use of the smallest possible mirrors allowed by diffraction, since there only needs to be room to hold one light beam. (In effect, all of the "bounces" are spatially superposed.) Not only is this the least demanding solution from the optics point of view, but it also simplifies the mechanical design of suspensions and vibration isolation systems (see below), compared with solutions based on multiple mirrors or single large mirrors. For this reason, it has been adopted by both Virgo and LIGO.

One measure of the effective number of bounces in a Fabry-Perot cavity is the storage time $\tau_s$, which is given by

$$\tau_s = \frac{L}{c} \frac{r_1}{1 - r_1}, \tag{14}$$

for an idealized cavity with perfect reflectivity at the end mirror and amplitude reflectivity coefficient $r_1$ for the input mirror.

There is, however, one major complication brought by the use of Fabry-Perot cavities, compared with systems that rely on discrete bounces off of mirrors. The "multi-pass" effect in a Fabry-Perot cavity comes from a resonance, and is only effective when the cavity length is very close to the precise resonance. This adds a major burden of *locking* to the process of controlling the interferometer: finding the resonance and then holding the arm sufficiently close to resonance.

In a Michelson interferometer whose arms are made of Fabry-Perot cavities, the response to a gravitational wave is a bit different from what we calculated above in Eq. 9. The response comes from the superposition of the responses of light that makes one round trip through the arm cavities with the light that makes two round trips, and with three round trips, etc. When we carry out the "phasor sum" of those responses, we find that

$$\Delta\phi = h\tau_s \frac{8\pi c}{\lambda} \frac{1}{\sqrt{1 + (4\pi f_{gw}\tau_s)^2}}. \tag{15}$$

If we choose an arm storage time longer than the period of gravitational waves of interest, then this can be approximated by

$$\Delta\phi \approx h\frac{2c}{\lambda f_{gw}}. \tag{16}$$

Thus, a small miracle has occurred, in that the cavity is automatically "optimized" for signals of all frequencies higher than the inverse of the storage time.

## 2.3  Shot noise

When the arm lengths of a Michelson interferometer are precisely matched, then the light beams return to the beam splitter with precisely the same phase. At the port away from the laser, there will be perfectly destructive interference. A departure from the condition of perfect match of arm lengths will cause some light to come out of that port, according to the law

$$P_{out} = P_{in}\sin^2\left(k_x L_x - k_y L_y\right). \tag{17}$$

Thus, an interferometer can be seen to be a transducer that converts a difference in light travel time between its two arms into a variable brightness at its output.

For reasons that will be explained below, it has proven best to operate interferometers at the "dark fringe" condition described above. However, it is pedagogically simpler to consider their operation at the seemingly more natural operating point at which the dependence of output power on arm length difference has the steepest slope. This is the point at which

half of the power emerges from the output port. At this operating point, the transduction coefficient is $dP_{out}/d\Delta L = (2\pi/\lambda)P_{in}$.

If one works at this operating point, then it is simple to see what is involved in looking for a gravitational wave: one looks for a small transient fluctuation in the amount of power emerging from the output point, and interprets it as a gravitational wave strong enough to result in such an output power change.

If only life were so simple! There can be other reasons for the power to fluctuate besides the passage of a gravitational wave through the apparatus. In this section, we will discuss several of the most important reasons for a false indication, or *noise.*

Firstly, let us consider the reason that is inherent in the character of light itself. For this purpose, the most important feature of light is that it consists of small chunks of energy called photons. For reasons that are too subtle to justify here, we can treat the arrival rate of photons at the beamsplitter as if each were an independent event. Thus, the statistics of the light beam are those of a Poisson distribution whose expectation value is $N_{mean}$ photons per second, where

$$N_{mean} = \frac{\lambda}{2\pi\hbar c}P_{out}. \tag{18}$$

In the large $N$ limit where gravitational wave interferometers work, a Poisson distribution approaches a Gaussian distribution, whose variance equals the mean $N_{mean}$.

What does this mean? The measurement of the output of the interferometer consists of making repeated short observations (on msec or sub-msec time scales) of the amount of light leaving the the output port, and interpreting the amount of light as an indication of the arm length difference in the interferometer. The inevitable fluctuations away from the "correct" amount of light are called *shot noise.* We have no choice but to interpret those quantum fluctuations of light power as if they indicated fluctuations in the arm length difference, and thus in the instantaneous value of $h(t)$. Thus, shot noise is a phenomenon that can obscure a signal that is too small compared with the amplitude of the noise.

Let's make an estimate of the amplitude of shot noise. If we carry through the above argument, we find that the standard deviation of a brief measurement of $h$ is given by

$$\sigma_h = \frac{1}{L}\sqrt{\frac{\hbar c\lambda}{4\pi P_{in}\tau}}, \tag{19}$$

equivalent to a white amplitude spectral density of

$$h_{shot}(f) = \frac{1}{L}\sqrt{\frac{\hbar c\lambda}{2\pi P_{in}}}. \tag{20}$$

To make shot noise sufficiently small, we need to illuminate the interferometer with a sufficiently powerful beam of light. One way to achieve this goal is to install a sufficiently powerful laser, but there is a less obvious trick that can help give the effect of a more powerful laser. Between the laser and the beam splitter of the interferometer, install a partially transmitting mirror, and adjust its position so that a resonance is set up for light making multiple round trips between this *power recycling* mirror and the light exiting the interferometer's beam splitter in the direction of the laser. Thus, one has created another Fabry-Perot cavity, called the recycling cavity, in which the role of the end mirror is played by the whole interferometer. To take full advantage of the possibility, one wants to pick as the interferometer's operating point not the mid-power point discussed above, but the *dark fringe* condition, in which all of the light leaving the beam splitter is directed back toward

the laser. Then, the resonant power recycling cavity gives the same effect as a laser whose power is greater than that of the laser itself by a number of order the finesse of the recycling cavity. This trick is too good not to use. Power recycling factors of order 50 have been used in Virgo and LIGO, while GEO600 used a power recycling factor of around 1000.[20]

(An alert reader will wonder how we can make observations with an interferometer operating at the dark fringe, where $dP/d\Delta L = 0$. The answer is to not keep it strictly at that operating point, but close to it. In initial interferometers, a small modulation about that operating point, at RF frequencies, is performed. In the steady state, the modulation only causes variations in output power at twice the modulation frequency, but when a signal is present it appears as a variation at the modulation frequency itself. One might still wonder about shot noise in this case, so far from the condition of maximum $dP/d\Delta L$. But here another small miracle occurs, and the shot noise limited sensitivity to $h$ is the same as at the naive operating point; heuristically, the smaller "signal" is compensated by a smaller level of light power fluctuations due to the proximity to the dark fringe. In advanced interferometers, a slight variation of this scheme will be used, with a small DC offset from the dark fringe taking the place of the RF modulation.[21])

In the presence of a gravitational wave, the "dark fringe" is not truly dark. A gravitational wave adds small *sidebands* to the laser light in the interferometer arms, and those sidebands emerge at the dark port. In a remarkably beautiful variation on the power recycling idea, one can install a partially transmitting mirror at the output port of the interferometer, and tune its location so that signal sidebands resonate in the interferometer.[22] This technique, called *signal recycling*, has been used at GEO, and will be a feature of advanced interferometers.

From the considerations discussed above, it would appear that the sensitivity of an interferometer will grow without limit as the laser power is increased. However, this flies in the face of our understanding from quantum mechanics that, at some level, the measurement process disturbs a physical system, thus setting a limit to the precision of measurements. It may not come as a surprise that, at the level of sensitivity to which we aspire in gravitational wave detection, the quantum limit can be important. The quantum limit is "enforced" by a competition between the shot noise limit to measurement precision and the fluctuating radiation pressure on the mirrors that also comes from shot noise.

A detailed discussion is subtle, and beyond the scope of this review. The quantum mechanical theory was first explained well by Caves.[23] Since what quantum mechanics limits is actually the product of measurement precisions in position and momentum, one can imagine that there might be a way to move below the shot noise limit in position sensitivity, at the cost of increased radiation pressure noise. The trick involves the use of *squeezed light.*[24] Tests have now been carried out to demonstrate that interferometer performance can be measurably improved by the use of squeezed light.[25]

## 2.4   Thermal noise

Shot noise is an example of a noise process that limits our ability to precisely read out the arm length difference in an interferometer. There are also a large class of noise effects that cause the arm length difference to actually vary, through motions of the mirrors caused by forces that are (in this context) less interesting than gravitational waves. Among these *displacement noise* effects, *thermal noise* plays a special role: it is one of the strongest noise sources, while at the same time being based on fundamental physics. It thus makes an instructive example for study.

Thermal noise is a generalization of the familiar phenomenon of *Brownian motion*. Discovered by Robert Brown around 1828, it remained a challenge to physical understanding for the rest of the 19th century.[26] The constant motion of microscopic particles suspended in water was suspected by some of suggesting a universal "vital force", while others guessed that it was indicative of random impacts on the visible particle from vast numbers of molecules of water. The latter school had the correct answer in mind, but no one could get the numbers to work out until Einstein found the right answer during his "miracle year" of 1905.[27] The successful explanation generated profound excitement; until then, there was no iron-clad proof of the existence of atoms, but an immediate result of Einstein's work was the determination of Avogadro's number, and thus of the mass of individual atoms.

In a gravitational wave interferometer, one can picture each of the (nearly) free mirrors as a very large Brownian particle. Their much greater mass means that Brownian motion will be very small, but effects that are small by any ordinary standard might still be important given the tiny size of mirror motions induced by realistic gravitational waves. The most direct analog of Brownian motion would be the motion induced by impacts of the gas molecules surrounding the mirrors. This is a prime reason to evacuate the space around the mirrors; at achievable vacuum levels, this noise source can be made negligible.

There is, however, a generalization of Brownian motion that turns out to be more important. The key physics is the recognition that many mechanisms can cause similar fluctuations, and that all of them can be recognized as intimately connected with dissipation of energy (such as mechanical friction, or electrical resistance, for example.) This is a deep insight, but is not necessarily surprising once one thinks of it; dissipation of energy involves the distribution of energy away from macroscopically observable degrees of freedom and into microscopic degrees of freedom. By coupling back to the macroscopic degree of freedom, those microscopic degrees of freedom are the source of fluctuations, which we can call generally *thermal noise*.

It might seem a hopeless task to account in detail for the dynamics of all of the different degrees of freedom into which energy might dissipate. Fortunately, that isn't necessary, because there is a powerful theorem that shows how little we need to know in order to calculate the level of thermal noise. This theorem is called the *Fluctuation-Dissipation Theorem*, one of the major results of non-equilibrium thermodynamics. It is expressed in a number of different forms, but for our purposes the most useful one comes from a series of papers by Callen and collaborators.[28]

The essential insight of the Fluctuation-Dissipation Theorem is that the strength of thermally-driven fluctuations is proportional to some suitable measure of the amount of dissipation in the system. The trick is to establish that "suitable measure". It proves useful to define, firstly, the complex quantity called the *impedance Z*, such that the equation of motion of the system of interest can be written in the frequency domain as

$$F_{ext} = Zv. \tag{21}$$

With a little study, it should be clear that this impedance is a generalization to the mechanical domain of the more familiar impedance in electrical systems. It is also useful to define the inverse of the impedance, called the *admittance Y*, such that

$$v = YF_{ext}. \tag{22}$$

With these definitions in hand, we can now state the Fluctuation-Dissipation Theorem. The power spectrum of the effective noise force applied to the system is

$$F_{therm}^2(f) = 4k_B T \mathrm{Re}(Z(f)). \tag{23}$$

Equivalently, the fluctuating motion of the system is characterized by a power spectrum of

$$x^2_{therm}(f) = \frac{k_B T}{\pi^2 f^2} \text{Re}(Y(f)). \tag{24}$$

How does this apply to a gravitational wave detector? We want to know how much the mirrors (playing the role of "free masses") will move. As described above, they will be resonantly suspended to allow them to behave freely at high frequencies, while remaining near the proper operating point at low frequencies. But in the context of thermal noise, we need to ask whether the suspension unavoidably brings in some dissipation that can drive thermal noise, even if we remove all external sources of dissipation such as air friction. It turns out that indeed there will always be dissipation whenever there is a suspension for the mass. The materials out of which a suspension is made always have an unavoidable level of *internal friction* that can come from a variety of mechanisms. (For a review of the physics involved, see [29].)

In the frequency domain, we can model internal friction as a modification of Hooke's Law, replacing the simple force law for a spring with

$$F = -k(1 + i\phi(f))x, \tag{25}$$

where the small imaginary fraction of the spring constant, $\phi$, encodes the phase lag between applied external force and response of the spring that is the embodiment of internal friction. For most materials, $\phi$ is a number of order $10^{-3}$, often roughly independent of frequency. (Note how different this is from dissipation from velocity friction, whose frequency dependence is proportional to one power of $f$.)

In terms of this model of dissipation, we can rewrite the power spectrum of thermal noise of a test mass as

$$x^2(f) = \frac{4k_B T k \phi}{2\pi f[(k - m(2\pi f)^2)^2 + k^2\phi^2]}. \tag{26}$$

This discussion of thermal noise from internal friction is necessary for understanding why a pendulum suspension has been the universal choice for all gravitational wave detectors built to date. A pendulum has a very special property: the "spring" that provides most of the restoring force on the mass is the gravitational force (through the tension in the wire.) Only a very small fraction come from elasticity in flexing pendulum wire. The gravitational/tensional spring constant is dissipationless; only the small extra spring constant from the flexing wire contributes its dissipation. The combination of the two springs is one effective spring whose loss fraction $\phi_{pend}$ is given by

$$\phi_{pend} = \phi_{wire} \frac{k_{el}}{k_{el} + k_{grav}}. \tag{27}$$

Thus, we can see that a pendulum suspension is a way to take a material with a given $\phi$ and "dilute" the dissipation to create a spring with a much lower $\phi$, and thus much lower thermal noise.[30]

In addition to the thermal noise from the pendulum mode, each degree of freedom adds its own thermal noise spectrum. The most important other degrees of freedom are those associated with internal vibrations of the mirrors, which form a spectrum starting at around 10 kHz. One can analyze these modes one-by-one, as with the pendulum mode. (Note that there is no dissipation dilution effect to help lower the noise.) The modal sum, averaged over

the intensity pattern of the laser beam spot on the mirror, gives the total of the effect.[31] Doing the modal sum correctly took genuine physical insight. An equivalent and elegant solution directly evaluates uses the Fluctuation-Dissipation Theorem without the need to analyze the mirror into modes of vibration.[32]

Fused silica has proven to be the best material to date for mirrors, not only possessing excellent optical properties but also remarkably low internal friction. Measured dissipation is typically $\phi \lesssim 10^{-6}$, and in some experiments as low as $10^{-8}$, at room temperature. (Note that in third-generation interferometers, in which cryogenics may be used to further reduce thermal noise, crystalline mirror substrates (perhaps silicon or sapphire) will need to be used instead, because glasses have much larger dissipation at low temperatures.)

When such good quality mirror substrates are used, the present limit on thermal noise comes from dissipation in the dielectric optical coatings on the front surfaces of the mirrors.[33] This is a subject of much current research. There are also other mechanisms besides direct motion of the mirror's surface that can couple thermal fluctuations into noise in the interferometer's output. See, for example [34]

## 2.5 Seismic noise

In his 1977 movie *Annie Hall*, the Woody Allen character Alvy Singer proposed that "life is divided into the horrible and the miserable". He defines "the horrible" by describing several categories of people especially deserving of pity, and then concludes that "the miserable is everyone else."[35]

Whatever the merits of this attitude toward the human experience, I would like to propose an analogous classification for sources of noise in physical measurements. Noise is divided into the fundamental and the ubiquitous. Fundamental noise sources are those like shot noise or thermal noise, that can be directly related to simple physical ideas, and whose strength can be calculated in specific circumstances from first principles. Ubiquitous noise sources are all of the others.

Of the ubiquitous noise sources, the strongest in gravitational wave interferometers may be seismic noise. Its ubiquity is unchallengeable – every part of the earth's surface shakes continually, by amplitudes of order 1 micrometer on time scales of seconds. Compared with the amplitude of expected gravitational wave signals, the seismic noise problem is enormous. It is also far from fundamental – I know of no way to link its strength to any fundamental physical principle.

The amplitude of seismic motion does vary from place to place on the earth's surface (and falls off with depth below the surface.) Nevertheless, one can say that a typical surface location might have a spectrum of

$$x(f) = 10^{-9} \mathrm{m}/\sqrt{\mathrm{Hz}} \tag{28}$$

at frequencies above 10 Hz.

If the test masses of an interferometer were to move with the spectrum of seismic noise, gravitational wave detection would be impossible. Fortunately, it is possible to *isolate* the masses. In this way, the problem may be substantially ameliorated, although not removed entirely.

One important and instructive aspect of seismic isolation is the pendulum suspension that is used to allow the test masses to respond "freely" to the effect of gravitational waves. This gives some freedom from the effects of seismic noise as well. The equation of motion

of a suspended mass is

$$m\ddot{x} = -k(x - x_g),$$ (29)

from which it is easy to see in the frequency domain that the transfer function is

$$\frac{x}{x_g} = \frac{f_0^2}{f_0^2 - f^2}.$$ (30)

(Inclusion of any form of damping in the model removes the infinity at $f = f_0$.)

Inspection of the transfer function reveals the basic idea of seismic isolation. For frequencies large compared with the resonance, the ratio of the motion of the mass to that of the ground is equal to $(f_0^2/f^2)$. At large enough frequencies, this isolation factor can be substantial.

This is great, but it is not a panacea. Firstly, note that the isolation is poor at frequencies just a bit above the resonance; not only that, but there is no isolation at all below the resonance, and there is amplification at and near the resonance. So isolation can only reduce the noise in a certain band of frequencies, with a more successful isolator being one with a lower resonance frequency.

Is the pendulum enough? No. It only starts to be enough at frequencies above 1 kHz. Things aren't even this good in reality. The model that we used in Eq. 30 above neglects the fact that the pendulum wire has some finite mass. If we were to include that effect in a more complete equation of motion, we would find a harmonic series of resonances (picturesquely called "violin modes") that cause amplification at each resonance. In typical interferometer designs, the fundamental violin mode comes at a few hundred Hertz.

Nevertheless, seismic isolation can save the day over a broad band of frequencies, so long as we use the same technique over and over. That is to say, we don't need to simply attach the top of our pendulums rigidly to the ground; instead, we can attach them to another mass that is itself resonantly suspended from another mass that is in turn resonantly suspended, and so on for as many stages as can be practicably engineered.

One classic kind of implementation is to have all of the stages above the test mass pendulum be made of conventional springs rather than pendulums. This gives the advantage of good compliance and isolation in the vertical direction, which an ordinary pendulum lacks.[36] Another possibility is to remedy the pendulum's vertical stiffness by adding carefully engineered vertical springs to the suspension point of the pendulum, and then repeating this kind of special pendulum multiple times. Virgo's SuperAttenuator is the most ambitious and successful isolator of this kind.[37]

Another ambitious way to dramatically reduce seismic noise is to use control systems to "actively" remove seismic noise. The basic idea is to equip a suspension platform with seismometers that measure its vibration in all degrees of freedom, and then to use feedback to reduce the level of vibration of the platform.[38] This approach to seismic isolation will be used in the Advanced LIGO interferometers.[39]

Seismic noise can also couple directly to test masses through the variation in the gravitational field caused by the changing distribution of matter in the local environment. When mechanical seismic isolation is successful enough at low frequencies, this *gravitational gradient noise* can be an important effect.[40]

## 2.6   Other ubiquitous noise sources

It may not come as a surprise that there are many other noise sources that affect an interferometer. In most cases, they are remote enough from fundamental ideas of physics that

we should categorize them as "ubiquitous." (The more standard name for this classification is "technical noise.")

There are several noises of optical origin beyond the fundamental shot noise. There can be excess intensity noise in a laser, beyond the level of shot noise. If the interferometer operating point is not strictly at the dark fringe point, this noise can be important. In addition, lasers unavoidably are subject to some fluctuations in the wavelength of their light. If the interferometer arms are not perfectly matched, such as for example in their arm lengths, then so-called *frequency noise* will appear in the output.

Frequency noise input to an interferometer is typically reduced by sending light from the laser through a *mode cleaning cavity* before it enters the interferometer. The mode cleaner also serves as an effective filter for angular "jitter" of the incoming laser light.

Most of the other ubiquitous noise sources are related to the various control systems that keep the interferometer aligned and held at its operating point. Crude position and angle control can be provided by local sensors on various parts of a test mass; a key function of these sensors is to provide a signal for feedback damping of the mirror suspension resonances. In addition, an interferometer may use several nested loops to control angles, with optical levers supplying large dynamic range for low frequency control but large noise, too; interferometric methods ("wavefront sensors") give quieter control at intermediate frequencies.[41] The length degrees of freedom need interferometric sensitivity levels to keep control noise from dominating the signals we seek.

A sample noise budget for the Virgo interferometer is shown in Figure 3.[42] The noise budget includes both fundamental and ubiquitous noise sources. At most frequencies, the noise was well understood, and near the design specifications. It is noteworthy how many non-negligible noise terms contribute to the observed noise spectrum. This is an indication of the challenging character of gravitational wave detection, as well as of the degree to which the challenge has been met.

# 3   State of the art

It took over thirty years from the time of Weiss's first design study for full-scale interferometers to come into existence and to observe the sky at the kinds of sensitivities that he envisioned. Finally, in the middle of the last decade, design sensitivity was reached by the largest interferometers.

The culmination of development work for first-generation interferometers came with a series of long observation runs. For initial LIGO, design sensitivity was attained in 2005, and thus an extended period of observation was embarked upon. Called Science Run 5 (or S5), its goal was to collect one year's worth of integrated triple coincidence observations among the three LIGO interferometers. It began on November 4, 2005 and ran until October 1, 2007. During this period, the GEO600 interferometer also participated in the S5 run.

Virgo commenced a long period of observation on May 18, 2007, overlapping with the LIGO and GEO data run; this was called Virgo Science Run 1 (or VSR1). By this time, LIGO and Virgo had agreed to jointly analyze their data (and to publish results together), so the start of VSR1 marks the beginning of observation by a global network of multi-km interferometers.

Each interferometer project carried out a set of upgrades after S5 and VSR1 finished, and then carried out further (mostly) joint observations. The LSC's S6 (from 7 July 2009 to 20 October 2010) and Virgo's VSR2 (7 July 2009 to 11 January 2010) and VSR3 (from
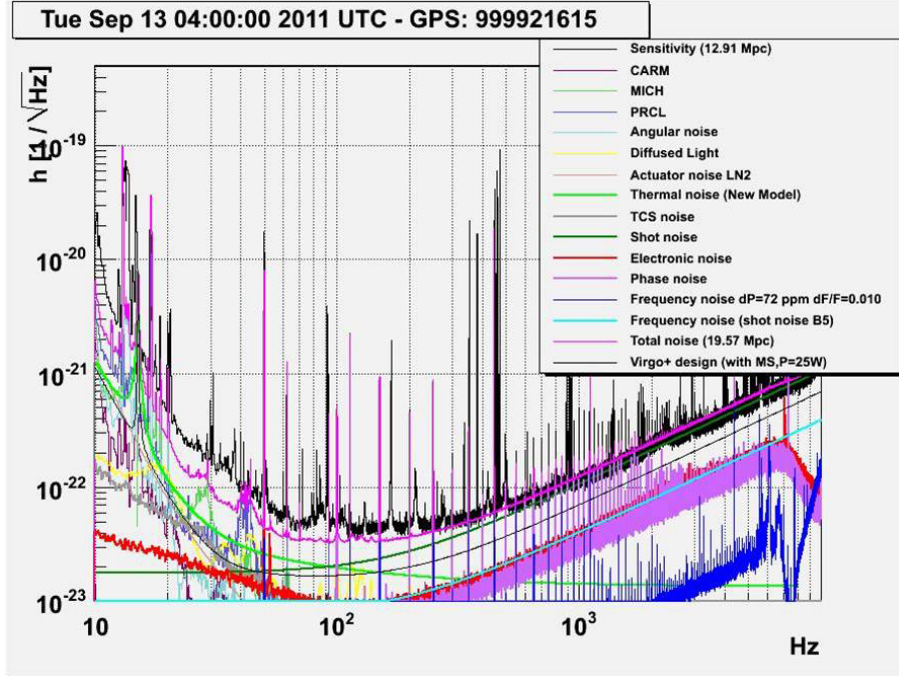
Figure 3: A recent noise spectrum of the Virgo interferometer. A wide range of noise sources contribute to the total noise, explaining the spectrum at most (but not all) frequencies.

11 August through 20 October 2010) were characterized both by improved performance and by the implementation of new technology serving as pathfinders for interferometers of the "advanced" or second generation period.

At the end of S6, the LIGO interferometers were shut down for decommisioning, to allow for the installation of Advanced LIGO. Virgo and GEO carried out further upgrades, and then joined for the S6e/VSR4 run, that began on June 3, 2011 and ran until 5 September 2011.

Looking ahead, LIGO and Virgo expect to begin operating their Advanced versions in the middle of the decade. The target sensitivity can be roughly characterized as a jump in strain sensitivity by an order of magnitude beyond that of the initial generation. This should be sufficient to allow for the detection of signals from neutron star binary systems (and perhaps many other sources), thus finally inaugurating the era of gravitational wave astronomy.

Here we review the features of the current generation of interferometers.

## 3.1 LIGO

The LIGO observatory[43] consists of three large interferometers at two sites, Hanford WA and Livingston LA. Two of the interferometers are installed at Hanford; during the period in question, one of them had arms of length 4 km, while the other had only 2 km arms. At Livingston, there is one interferometer of 4 km arm length. The LIGO Laboratory, located at Caltech and MIT, operates these facilities. The scientific program is carried out by the LIGO Scientific Collaboration, consisting of over 800 members at institutions across the United States and in many other countries.

The optical configuration of a LIGO interferometer can be summarized as follows: The main interferometer is a Michelson interferometer whose arms are Fabry-Perot cavities with finesse = 220. The interferometer is illuminated by a Nd:YAG laser with output power of 10 W. A power recylcing mirror allows a resonant enhancement of laser power by a factor of about 50. Between the laser and the power recycling mirror, a resonant cavity called a *mode cleaner* performs both spatial filtering ("mode cleaning") and frequency stabilization.

Test masses were fused silica cylinders 25 cm diameter by 10 cm thick, with a mass of 10.7 kg. They were suspended by a single loop of steel wire, with a resonant frequency of 0.76 Hz. Thermal noise from the pendulum mode of the test mass suspensions was dominated by the internal friction in the steel wire loops, as "diluted" by the gravitational effect described above.

This pendulum suspension was in turn hung from a four-layer mass-spring isolator (or "stack") with resonant frequencies near 10 Hz. The combined isolation of pendulum and isolation stack was about $10^{12}$ at 100 Hz, but only a few orders of magnitude at 10 Hz; thus, a steep "seismic wall" dominated the low frequency portion of the noise spectrum.

Figure 4 shows the noise spectrum that was achieved in the Hanford 4 km interferometer during S5, along with the noise budget as expressed by spectra of the major known contributors. At high frequencies, shot noise explains the spectrum very well, with "technical" noise sources well under control. In the region of lowest noise, just above 100 Hz, shot noise is joined by thermal noise from the mirrors, thermal noise in the pendulum mode, and noise in the length-control system. Between 40 and 100 Hz, all of the above contribute, with the exception of shot noise, but there is a gap (of order a factor of two) between the measured noise and the contributions of all known noise source. The reason for this gap is not understood. Below 40 Hz, seismic noise is one of the main contributors, but is joined at comparable levels by noise in both the length control and in the angle control systems.

One useful scalar measure of the noise is the neutron star binary *horizon distance*, the maximum distance to which a signal from an optimally oriented binary system of two 1.4 $M_\odot$ neutron stars could be detected at a signal-to-noise ratio of 8. During the S5 run, the LIGO 4 km interferometers achieved horizon distances of approximately 30-35 Mpc.

One other feature of the noise must be stressed. The noise power spectrum characterizes the level of the steady Gaussian noise in the interferometers. At some frequencies (especially above 200 Hz where shot noise dominated), this fully characterizes the noise. However, at lower frequencies, an additional noise component appeared in the form of frequent non-Gaussian "glitches". The causes of these glitches were highly varied; some were tracked down to specific faults and fixed; other glitches showed strong statistical correlations with various internal degrees of freedom, but could not be explained in detail. A few glitch phenomena remained entirely mysterious. The importance of this non-Gaussian behavior depended on how the data was being analyzed; searches for steady effects (for signals from pulsars or for a stochastic background) were hardly affected at all, while searches for transient signals had to go to some lengths to minimize the problems caused by glitches masquerading as gravitational wave signals. The search for signals from compact binary coalescences could take advantage of detailed knowledge of the expected waveforms to develop techniques that largely (although not entirely) removed the deleterious effects of glitches; on the other hand, the search for transients of unknown form (the "burst" search) was dramatically affected in its sensitivity by the level of glitchiness of the data. A number of clever diagnostic techiques were developed to aid in the hunt for the causes of glitches, but one suspects that some level of understanding still eluded the team.[44]

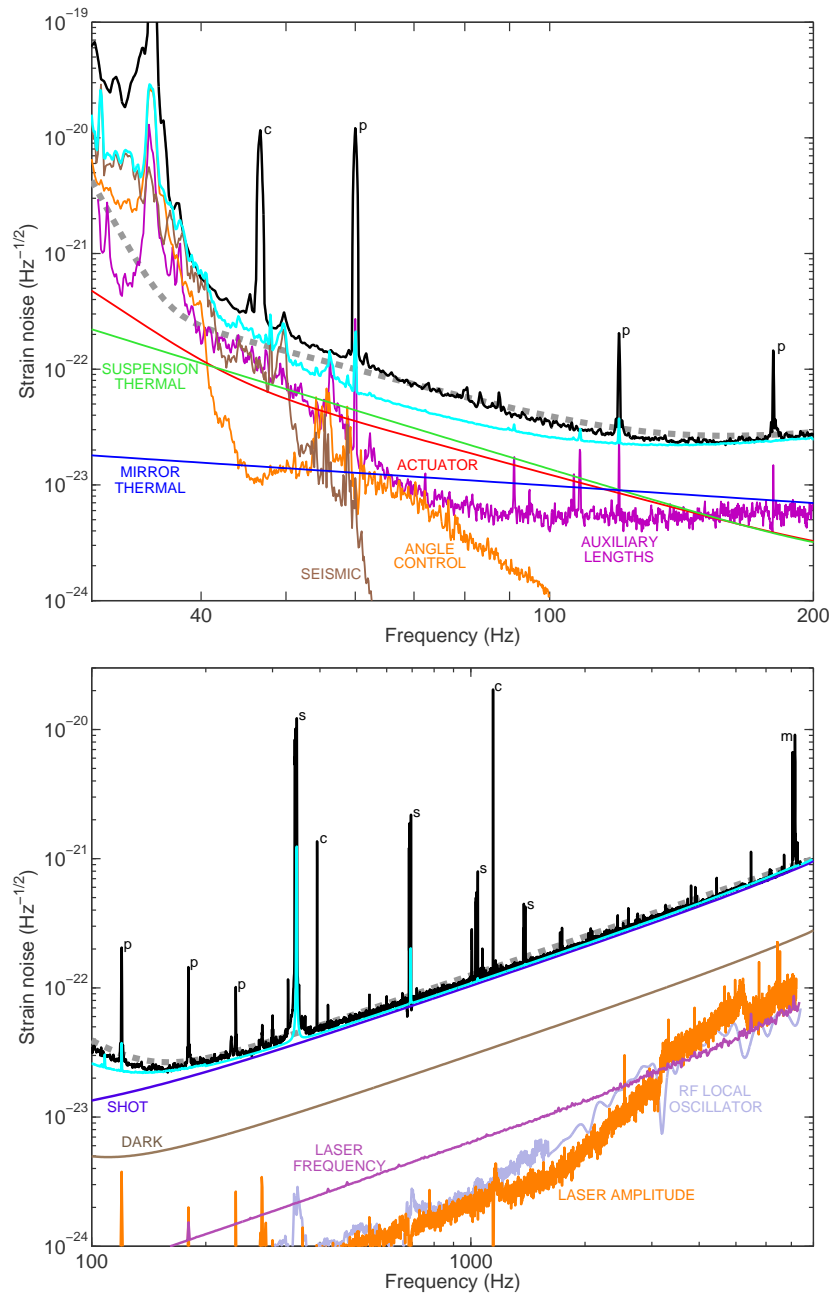Before the S6 run, several changes were made. The original 10 W laser was swapped out

Figure 4: Noise performance of the Hanford 4 km interferometer during S5, with the contribution of known noise sources. The blue curve shows the sum of all of the known noise sources, while the black curve shows the measured noise spectrum. The good match between those curves demonstrates that at most frequencies (but not all), the noise model gave a good explanation of the observed performance. The noise met the design goals (shown in the gray dashed line) at all frequencies down to about 60 Hz.
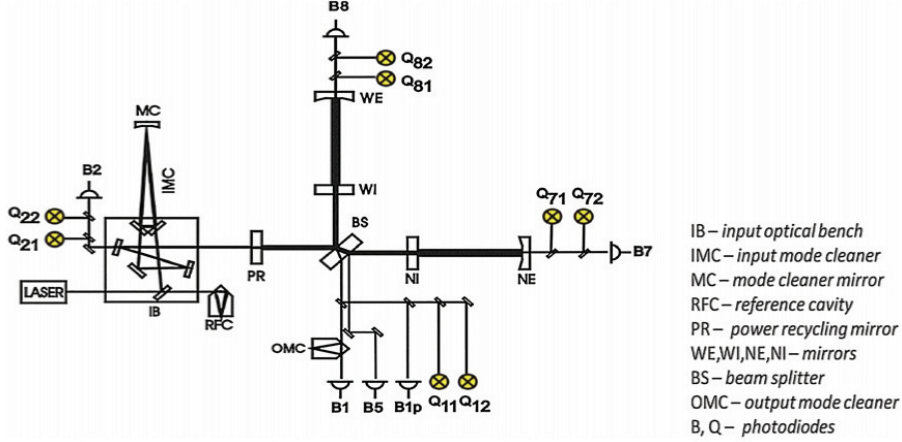
Figure 5: Optical schematic diagram of the Virgo interferometer

in favor of a 35W laser that forms the core of the Advanced LIGO laser. (The aLIGO laser will reach 200 W with an additional amplifier stage.) An output mode cleaner was added, to reduce the amount of "junk" (non-$TEM_{00}$) light reaching the output photodiodes; this also enabled a change in the interferometer demodulation scheme from the classic RF readout to DC readout. Both of these changes were also pathfinders for aLIGO technology. As a result of these changes, high frequency noise was reduced by about a factor of 2, as expected for shot noise.

## 3.2  Virgo

The Virgo interferometer[45] is a 3km long power-recycled Fabry-Perot Michelson, located at Cascina, Italy (near Pisa.) Its optical system is shown in Figure 5.

Perhaps the most distinctive feature of the Virgo interferometer is its use of an ambitious, carefully-engineered seismic isolation system as an integral part of the design. Each of the six key mirrors (end mirrors of the arm cavities, beam splitter, and power recycling mirror) is suspended from a 7.3 m tall isolation and suspension system called a *superattenuator*, as shown in Figure 6. At its heart is a chain of pendulums, each stage of which provides good attenuation in the vertical direction as well as in the "natural" horizontal directions. This is supplemented by a tall inverted pendulum providing one stage of very low frequency isolation. The combined effect is a factor of $10^{15}$ of seismic isolation at 10 Hz. Thus, Virgo has been able to achieve unparalleled sensivity at low frequencies, as compared with other interferometers (like LIGO) with more modest isolation systems.

After VSR1, several upgrades were made. In addition to the installation of lower-noise electronics and upgrades to the input optics, a thermal compensation system was installed to allow the use of higher laser power. Together, these allowed substantial improvements in the sensitivity during VSR2 as compared with VSR1. The range for detection of neutron star binaries increased from around 8 Mpc to about 20 Mpc. Between VSR2 and VSR3, a second upgrade focused on replacing steel-wire test mass suspensions with a "monolithic" all-fused-silica suspension to reduce pendulum thermal noise. This is an important pathfinder for advanced interferometer technology. Unfortunately, optical problems with the new mirrors caused a mismatch in cavity parameters that led to excess optical noise. Commissioning
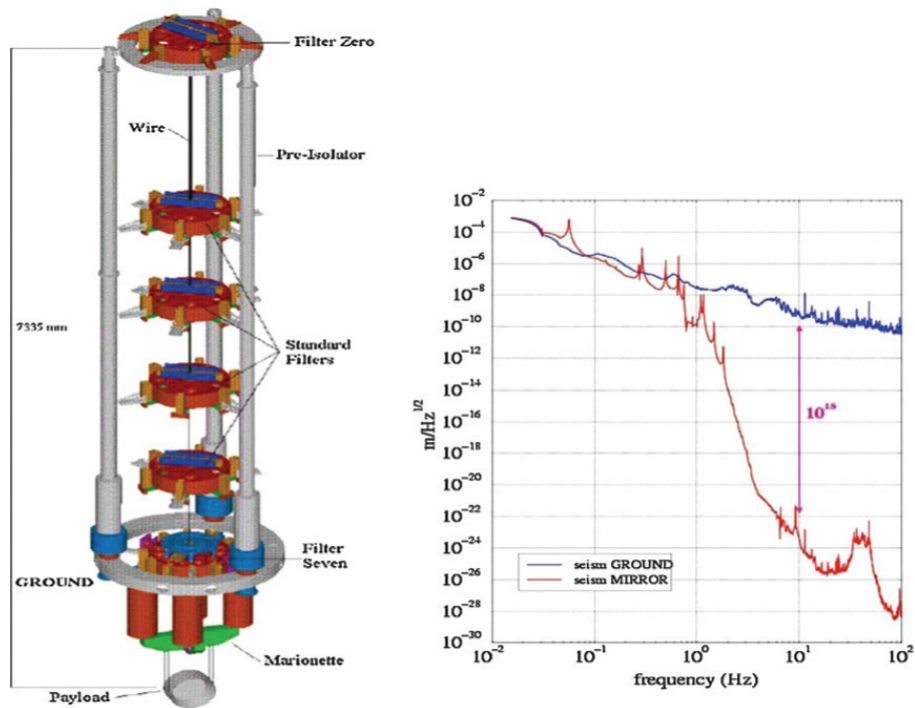
Figure 6: (Left) A rendering of the Virgo Super Attenuator, the most successful seismic isolation system yet implemented in a gravitational wave interferometer. (Right) The seismic noise spectrum at Virgo (blue), and the transmitted noise spectrum (red), demonstrating the performance of the Super Attenuator.

after VSR3 focused on a heating system to match the mirrors' radii of curvature. The result was substantially improved performance, as indicated by the increase of NS binary inspiral range to close to 30 Mpc for the VSR4 run. [42]

## 3.3 GEO600

The GEO600 interferometer[46] is a power- and signal-recycled simple Michelson interferometer with 1200 m arms, folded once to fit in a 600 m site in Ruthe (near Hannover), Germany. It is operated by the German-British GEO Collaboration; all members of GEO are members of the LIGO Scientific Collaboration, and GEO600 is operated as an LSC detector, along with the Hanford and Livingston interferometers in the USA.

GEO600 made the most of its short length by focusing aggressively on "advanced" technologies. These included early implementation and study of signal recycling and, more recently, the use of squeezed light. In addition, GEO600's design included high-$Q$ all-fused-silica ("monolithic") test mass suspensions, controlled by "reaction masses" isolated in a parallel chain. The isolation system itself bears conceptual similarity to that of Virgo, in that it contains several stages in which vertical compliance rivals the compliance in the horizontal directions. Some of these systems (especially the fused silica suspensions) served as rather direct prototypes for the designs adopted for Advanced LIGO.

Because of its shorter arms and its lack of Fabry-Perot cavities or other means of multiple bounces, it was never expected that GEO600 would reach the same levels of sensitivity at low frequencies as the LIGO or Virgo interferometers. Nevertheless, GEO600 has been quite successful. At high frequencies (above 1 kHz), it has reached sensitivities comparable to that of the Virgo interferometer and of the 2 km LIGO interferometer at Hanford. GEO600 operation has also set the pace for stability, typically achieving data collection duty factors in excess of 90%.

GEO600 joined the S5 run on 21 January 2006, acquiring data first during nights and weekends while commissioning continued in regular working hours. Between May 1 and October 6, 2006, it collected data full time, then switched back to night/weekend data collection for the remainder of S5. During S6 it functioned in night/weekend data collection mode. It teamed with Virgo for the S6e/VSR4 run.

## 4    The next generations of interferometers

With the end of S6, LIGO's interferometers were shut down and then removed from the Hanford and Livingston facilities to allow for the installation of Advanced LIGO. Virgo remained operating until 5 September 2011 in the VSR4 run, in coincidence with GEO600 (which called the run S6e.) Since that date, Virgo and GEO have been devoted to major upgrades, Virgo toward Advanced Virgo, and GEO toward GEO-HF.

## 4.1    aLIGO

Advanced LIGO (or aLIGO)[47] will be an entirely new set of interferometers at the two LIGO sites. The buildings and vacuum systems will remain, but everything else is being replaced. Such a radical change was necessary to allow an intended order of magnitude increase in sensitivity at 100 Hz and above, along with an extension of the senstive frequency band downward from  40 Hz in initial LIGO to about 10 Hz in aLIGO. Figure 7 shows the design goals.
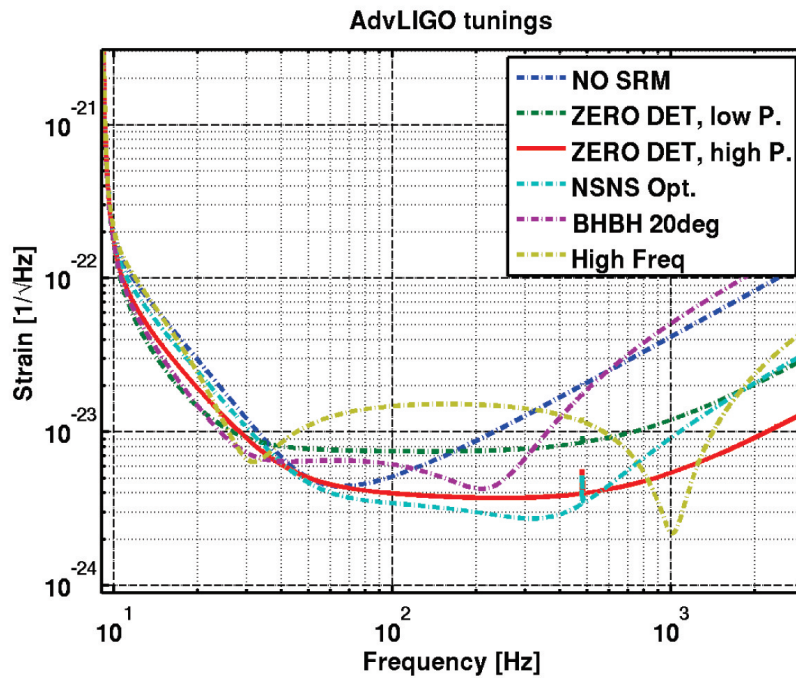
Figure 7: Anticipated noise spectra of Advanced LIGO in various configurations. The dark blue curve and the dark green curve show the noise expected in two possible early low power configurations, without (blue) and with (green) signal recycling. The other curves show different possible tunings of the complete Advanced LIGO system, optimized for different signals.

To achieve such a dramatic improvement in performance, major features of the interferometer have been changed from their S5 implementations (and in most cases from S6 as well.) The most important features will be:

- laser power upgrades (S6 reached 35 W; aLIGO will eventually use about 200 W.)

- signal recycling to tailor the spectrum of the shot noise in the middle and high frequency bands

- 40 kg mirrors made of best quality fused silica, with fused silica suspensions and optimized coatings, aimed at reduction of internal thermal noise

- a completely new vibration isolation system, including two stages of "active" vibration isolation, along with several additional stages of soft passive isolation.

Current schedules call for a science run of aLIGO at good sensitivity in 2015.

## 4.2  Advanced Virgo

Virgo has several head starts over LIGO in the implementation of advanced technology. From the start, it has had outstanding vibration isolation. In addition, a monolithic fused silica suspension system was installed in the upgrade between VSR2 and VSR3. Thus, there are fewer dramatic changes necessary to move toward second-generation performance.

The design goal for Advanced Virgo[48] is to achieve a factor of 10 improvement in noise levels over the initial Virgo design, over a frequency band from 10 Hz to 10 kHz. To achieve that, the changes will not be inconsiderable. Laser power will eventually have to grow to around 200 W. To minimize radiation pressure noise, mirror mass will increase to about 40 kg. Signal recycling will be implemented. A new beam injection system, equipped with sophisticated active seismic isolation, will be implemented.

Installation of Advanced Virgo begins in October 2011. The present schedule calls for completion of installation and testing, to the point of robust locking of the interferometer, by the end of 2014.

## 4.3  GEO-HF

GEO-HF[49] is the name given to a program of gradual upgrades to the GEO detector, aimed at increasing the sensitivity beyond what was achieved by GEO600 through the S5 science run. Starting with the period of the S6 run, the GEO team began a set of upgrades that includes tuned signal recycling and DC readout, implementation of an output mode cleaner, and the implementation of squeezing.[50] Continued improvements will be made to the optical parameters, including increased laser power, with the eventual aim of about one order of magnitude improvement in the noise level at frequencies above 1 kHz.

During this program of improvements, GEO-HF will collect data during nights and weekends. This is especially important since there will be a period of several years (until 2015) when both LIGO and Virgo will be "off the air" for the installation and commissioning of the advanced interferometers.

## 4.4 LCGT

The Large-scale Cryogenic Gravitational wave Telescope (LCGT)[51] project got under way recently in Japan. It aims at the construction of a 3 km interferometer deep underground at Kamioka. The underground site provides dramatically lower seismic noise than a surface site. Another key design goal of LCGT is to make use of cryogenics to lower the contributions of thermal noise to the overall noise budget. Because fused silica gets very lossy at low temperatures, LCGT will use sapphire substrates for its mirrors. Both underground installation and cryogenic operation are likely features of next-generation interferometer designs, so confronting these challenges early will allow LCGT to play the role of pathfinder for these technologies.

The project expects to start construction of its tunnels and vacuum systems soon; however, the disastrous earthquake of 11 March 2011 has injected some uncertainty into the schedule. The most recent plans call for an interferometer of more conventional technology (room temperature, silica optics, low power laser, and less ambitious seismic isolation) to be installed first, later to be replaced by the more advanced interferometer. Still, it is hoped that observations with the advanced interferometer can begin in 2017.[52]

## 4.5 Beyond the "Advanced" Era

The "Advanced" detectors are confidently expected to achieve the sensitivity required to start finding gravitational wave signals. This will be an exciting time for the field. It will mark the inauguration of a new branch of astronomy, as well as a new probe for gravitational physics.

Almost certainly, there will be a demand for yet more sensitive observations, so that more signals can be studied at higher signal-to-noise ratios. The recognition of this has led to some initial studies of ideas for a generation of instruments to succeed those now under construction.

By far the most serious and detailed study of next-generation interferometers has been carried out by the Einstein Telescope project.[53] Carried out by a team of experts from across Europe, the 2010 conceptual design for ET envisions an underground site equipped with three 10 km long interferometers in a triangular configuration. Cryogenic technology will be used to reduce thermal noise. Quantum noise reduction strategies also play an important role in reaching the foreseen order of magnitude improvement in sensitivity beyond the Advanced interferometers.

## Acknowledgments

## References

[1] A. Einstein, Preussische Akademie der Wissenschaften, Sitzungsberichte, 1918 (part 1), 154167 (1918)

[2] D. Kennefick, *Traveling at the speed of thought: Einstein and the quest for gravitational waves* Princeton: Princeton University Press (2007) 319 pp.

[3] A. S. Eddington, Proc. R. Soc. Lond. A **102**, 268 (1922)

[4] A. Einstein and N. Rosen, Jour. Frank.Inst. **223**, 43 (1937)

[5] H. Bondi, Nature **179**, 1072 (1957)

[6] B. DeWitt and C. M. DeWitt *Proceedings of conference at Chapel Hill, North Carolina, January 18-23, 1957* (Wright Air Development Center technical report 57-216, United States Air Force, Wright-Patterson air force base, Ohio, (1957))

[7] F. Pirani, Acta Phys. Polon. **15**, 389 (1956); F. Pirani, Phys. Rev. **105**, 1089 (1957)

[8] P. Saulson, Gen. Relativ. Gravit. DOI 10.1007/s10714-011-1237-z

[9] R. Weiss, Quarterly Progress Report of the MIT Research Laboratory of Electronics, No. 105, pp. 54-76 (1972). Other early pioneers included G. E. Moss, L. R. Miller, and R. L. Forward, Appl. Opt. **10** 2495 (1971); for a more complete history, see P. R. Saulson in A. Ashtekar, ed., *100 Years of Relativity: Space-Time Structure: Einstein and Beyond* Singapore: World Scientific (2005), pp. 228-256.

[10] B. Schutz and M. Tinto, M.N.R.A.S. **224**, 131 (1987)

[11] S. Klimenko, S. Mohanty, M. Rakhmanov, and G. Mitselmakher, Phys. Rev. D **72**, 122002 (2005)

[12] S. Chatterji, A. Lazzarini, L. Stein, and P. J. Sutton, Phys. Rev. D **74**, 082005 (2006)

[13] The LIGO Scientific Collaboration and the Virgo Collaboration, Class. Quant. Grav. **27** 173001 (2010)

[14] P. R. Saulson, *Fundamentals of Interferometric Gravitational Wave Detectors*, Singapore: World Scientific (1994) 300 pp.

[15] J. D. E. Creighton and W. Anderson *Gravitational-Wave Physics and Astronomy: An Introduction to Theory, Experiment and Data Analysis* Weinheim, Germany: Wiley - VCH (2011) 375 pp.

[16] A. A. Michelson and E. W. Morley, Am. J. Sci. **34**, 333 (1887)

[17] A. A. Michelson, Am. J. Sci. **22**, 120 (1881)

[18] R. W. P. Drever et al., in E. Schmutzer, ed., *Proceedings of the Ninth International Conference on General Relativity and Gravitation(Jena 1980)* Berlin: VEB Deutscher Verlag der Wissenschaften (1983) p. 256

[19] D. Herriott, H. Kogelnik, and R. Kompfner, Appl. Opt. **3**, 523 (1964)

[20] R. W. P. Drever, in N. Deruelle and T. Piran, eds., *Gravitational Radiation* Amsterdam: North Holland Publishing (1983), p. 321

[21] P. Fritschel, LIGO-G030460, http://www.ligo.caltech.edu/docs/G/G030460-00/G030460-00.pdf; R. L. Ward et al., Class. Quantum Grav. **25**, 114030 (2008); S. Hild, et al., Class. Quantum Grav. **26** 055012 (2009)

[22] B. J. Meers, Phys. Rev. D **38**, 2317 (1988)

[23] C. M. Caves, Phys. Rev. Lett. **45**, 75 (1980)

[24] D. F. Walls, Nature **306** 141 (1983)

[25] The LIGO Scientific Collaboration, Nature (Physics) doi:10.1038/nphys2083 (2011)

[26] D. K. C. MacDonald, *Noise and Fluctuations: An Introduction* New York: Wiley (1962)

[27] A. Einstein 1905, Annalen der Physik **17**, 549 (1905)

[28] H. B. Callen and T. A. Welton, Phys. Rev. **83**, 34 (1951); H. B. Callen and R. F. Greene, Phys. Rev. **86**, 702 (1952)

[29] C. Zener, *Elasticity and Anelasticity of Metals*, Chicago: University of Chicago Press, 1948; A. S. Nowick and B. S. Berry, *Anelastic Relaxations in Crystalline Solids*, New York: Academic Press, 1972

[30] P. Saulson, Phys. Rev. D **42**, 2437 (1990); G. González, Class. Quantum Grav. **17**, 4409 (2000)

[31] A. D. Gillespie and F. J. Raab, Phys. Rev. D **52**, 577 (1995)

[32] Y. Levin, Phys. Rev. D **57**, 659 (1998)

[33] G. M. Harry, H. Armandula, E. Black, D. R. M. Crooks, G. Cagnoli, J. Hough, P. Murray, S. Reid, S. Rowan, P. Sneddon, M. M. Fejer, R. Route, and S. D. Penn, Appl. Opt. **45** 1569 (2006).

[34] V. B. Braginsky, M. L. Gorodetsky, and S. P. Vyatchanin, Phys. Lett. A **271** 303 (2000); Y. Levin, Phys. Lett. A **372** 1941 (2008)/

[35] http://www.imdb.com/title/tt0075686/quotes

[36] J. Giaime, P. Saha, D. Shoemaker and L. Sievers, Rev. Sci. Instrum. **67** 208 (1996)

[37] S. Braccini et al., Rev. Sci. Instrum. **67** 2899 (1996); S. Braccini et al., Rev. Sci. Instrum. **64**, 310 (2009)

[38] S. J. Richman, J. A. Giaime, D. B. Newell, R. T. Stebbins, P. L. Bender and J. E. Faller, Rev. Sci. Instrum. **69**, 2531 (1998)

[39] R. Abbott, et al., Class. Quantum Grav. **19**, 1591 (2002)

[40] S. A. Hughes and K. S. Thorne, Phys. Rev. D **58**, 122002 (1998); M. Beccaria et al., Class. Quantum. Grav **15** 3339 (1998); T. Creighton, Class. Quantum Grav. **25** 125011 (2008).

[41] E. Morrison, B. J. Meers, D. I. Robertson, and H. Ward, Appl. Opt. **33**, 5041 (1994); Y. Hefetz, N. Mavalvala, and D. Sigg, J. Opt. Soc. Am. B **107**, 1597 (1997)

[42] E. Calloni, https://dcc.ligo.org/cgi-bin/private/DocDB/ShowDocument?docid=71008

[43] B. P. Abbott et al. (The LIGO Scientific Collaboration), Rep. Prog. Phys. **72** 076901 (2009)

[44] L. Blackburn et al., Class. Quantum Grav. **25**, 184004 (2008); N. Christensen for the LIGO Scientific Collaboration and the Virgo Collaboration, Class. Quantum Grav. **27**, 194010 (2010); J. Slutsky et al., Class. Quantum Grav. **27**, 165023 (2010)

[45] T. Accadia et al. Class. Quantum Grav. **28**, 114002 (2011)

[46] H. Grote for the LIGO Scientific Collaboration, Class. Quantum Grav. **25**, 114043 (2008)

[47] G. M. Harry for the LIGO Scientific Collaboration, Class. Quantum Grav. **27**, 084006 (2010)

[48] The Virgo Collaboration, *Advanced Virgo Baseline Design* VIR-027A-09, https://tds.ego-gw.it/itf/tds/index.php?callContent=2&callCode=6616

[49] H. Grote for the LIGO Scientific Collaboration, Class. Quantum Grav. **27**, 084003 (2010)

[50] H. Grote, LIGO-G1100999, https://dcc.ligo.org/cgi-bin/private/DocDB/ShowDocument?docid=70888

[51] K. Kuroda for the LCGT Collaboration, Class. Quantum Grav. **27**, 084004 (2010)

[52] E. Hirose for the LCGT Collaboration, LIGO-G1101057 https://dcc.ligo.org/cgi-bin/private/DocDB/ShowDocument?docid=71004

[53] S. Hild et al., Class. Quantum Grav. **28**, 094013 (2011); S. Aoudia, et al., (The ET Science Team), *Einstein gravitational wave Telescope conceptual design study*, ET-0106A-10 (2010), http://dl.dropbox.com/u/18549909/et-design-study.pdf